

Chapter 5

Surface SHG from Cr-SiO₂-Si(001) structures

5.1 Introduction

Silicon is the dominant semiconductor material for electronic circuits and devices. Ongoing miniaturization of electronic systems drives critical regions of integrated circuits ever closer to silicon interfaces. SiO₂-Si interfaces are of particular importance due to their almost ubiquitous presence in metal-oxide-semiconductor (MOS) structures and MOS field-effect transistors. The thickness of the gate insulator (commonly SiO₂) for MOS transistors is being scaled down. However, there exists a scaling limit because tunneling current through the gate oxide increases drastically with reduced thickness. In addition, dopants may penetrate from the heavily doped polysilicon gate into the substrate, which causes instability in the threshold voltage. Performance and reliability of MOS structures depends more and more on the microscopic quality of dielectrics and their interfaces. Traditionally, the properties of SiO₂-Si interfaces were investigated by means of electrical characterization, such as capacitance voltage (C-V), current voltage (I-V) and constant voltage stress (I-t) measurements [73, 74]. The nonlinear optical method of second-harmonic generation (SHG) has been developed into a sensitive surface or interface probe [19, 20, 54]. Among the many advantages of this technique, the features of non-contact sampling and accessibility to buried interfaces are most attractive to the microelectronics industry. It has been shown that surface SHG is sensitive to a number of properties of

the SiO₂-Si interface, such as crystalline orientation [24], interfacial structure [33, 75], preparation and roughness [57, 58], and charge transfer [66, 76].

The Cr-SiO₂-Si(001) structures have been used to study the SHG dependence on the bias dc field across the SiO₂-Si interface [37, 69-71], but the sources of SHG in reflection from such complicated MOS structures were not systematically investigated. It was found that the SHG signals produced in reflection from silicon or silver surface showed a significant variation with a dc bias electric field applied normal to the surface [77]. The dc field was applied by immersing the sample in an electrolyte solution with a bias voltage between it and an electrode. SHG at the SiO₂-Si interface was also found to be very sensitive to a dc field across the interface. The enhancement of SHG is caused by the electric-field-induced SHG (EFISH) effect. In the original experiment on the EFISH effect at the SiO₂-Si interface [36], the dc field was applied between the Si substrate and a ring shaped metal electrode on top of the SiO₂ layer, and SHG was measured in transmission geometry through the metal ring; therefore, the propagation of light was not affected by the electrode. Several further EFISH experiments were performed on Cr-SiO₂-Si structures using a reflection geometry [37, 69-71]. In these studies, the dc biases were applied between the Si substrate and an ultrathin semitransparent Cr film, which fully covered the SiO₂ layer, so the incident light was transmitted through the Cr coating film to reach the SiO₂-Si interface. The measured SHG signals and the bias dependent SHG spectroscopy were treated as if they came from the SiO₂-Si interface alone with no contribution from the Cr coating. With the experimental evidence for high sensitivity of SHG to surface conditions, it is reasonable to question the pre-condition that the SHG signal in

reflection from such a Cr-SiO₂-Si(001) structure has negligible contribution from the Cr coating film. Several regions of the MOS structure, such as the outer surface of the Cr film, the Cr-SiO₂ interface, or even the SiO₂ or Cr bulk, could be possible SHG sources. The experimental evidence of strong enhancement of SHG at metal surfaces by a dc bias [77] also suggests that the SHG bias dependence could come from the Cr-SiO₂ interface as well.

In this chapter, we present a comprehensive study of the effect of ultrathin Cr coating film on the SHG response in reflection from the Cr-SiO₂-Si(001) MOS structures. In addition, we study the influence of the thickness of the SiO₂ layer on the SHG response. The aims of this work are to identify the sources of SHG from MOS structures and to explore the potential for using the surface SHG to characterize the electronic dynamics in MOS structures. We compare SHG signals from Cr coated and uncoated SiO₂-Si surfaces and compare SHG signals from thin oxide and thick oxide covered Si surfaces in several respects, including rotational-anisotropy SHG (RA-SHG), SHG spectroscopy, and time-dependent SHG (TD-SHG). We find that the RA-SHG peak locations (azimuthal angles) of the RA-SHG signals from Cr coated and uncoated SiO₂-Si surfaces differ at higher photon energies but are the same at lower photon energies for several polarizations. The modulation of peaks and valleys in RA-SHG signals arises from interference between isotropic and anisotropic SHG contributions (see Chapters 3 and 4), whereas the anisotropic contribution is generated only from the bulk and is independent of surface preparation. Therefore, RA-SHG signals carry phase information about the surface SHG relative to the bulk anisotropic SHG. The altered peak location of the RA-SHG signals indicates that the

Cr layer on oxidized Si(001) surfaces produces an additional SHG contribution compared to uncoated surfaces. The strength of SHG contribution originated from the Cr coating varies with photon energy. The observed SHG signal from the Cr coated natively oxidized Si surface is weaker than the Cr coated thermally oxidized Si surface; but this relation is reversed for samples before the Cr coating. The observed TD-SHG signals decrease with time for Cr coated SiO₂-Si surfaces while increase for uncoated surfaces. To further identify the additional sources of SHG, we investigate SHG from the surface of a very thick Cr film and from the SiO₂-Cr interface with and without a dc bias. We show that SHG contributions from all these surfaces (or interfaces) are non-negligible at certain photon energies. We attribute the difference in the SHG spectrum from Cr coated and uncoated samples to interference between additional and original SHG contributions.

5.2 Theoretical background

From the phenomenological theory in Chapter 2, both bulk and surface contribute to the SHG. We take advantage of this natural co-existence of bulk and surface SHG and show that we can actually obtain reliable phase information for surface SHG, which can be easily utilized to distinguish different surface conditions. This is realized by combining polarization selection and RA-SHG. The fact that the bulk anisotropic SHG can be independently detected from the Si(001) face makes it a good choice for studying surface SHG.

From Chapter 2, the h -polarized SHG fields $E_{g,h}^{(2\omega)}$ are related to the g -polarized incident fundamental fields E_g by,

$$E_{g,s}^{(2\omega)} = a_{4,(g,s)} \sin(4\phi) e^{i\delta_{g,s}} E_g^2, \quad (5.1)$$

$$E_{g,p}^{(2\omega)} = [a_{0,(g,p)} + a_{4,(g,p)} \cos(4\phi)] e^{i\delta_{g,p}} E_g^2, \quad (5.2)$$

where ϕ is the azimuthal angle measured between the plane of incidence and the [100] axis in the surface. The coefficients a_n 's are functions of related susceptibility tensors elements and linear optical factors (see Chapter 2). Here, the polarization (g or h) of both fields is limited to be s or p .

On the other hand, for a special polarization (q, s), for which the bulk and surface SHG can be exactly separated in theory, this relation takes the form,

$$E_{q,s}^{(2\omega)} = [a_{0,(q,s)} + a_{4,(q,s)}^s \sin(4\phi) + a_{4,(q,s)} \cos(4\phi)] e^{i\delta_{q,s}} E_q^2. \quad (5.3)$$

The SHG intensity is proportional to the magnitude squared of the SHG field. If the anisotropic coefficient, a_4 , is chosen to be positive and real (with its phase included in $\delta_{g,h}$), then the isotropic term, a_0 , is complex in general. As shown in Chapter 2, if the γ SHG contribution is neglected, all other tensor elements can be determined from polarization selected RA-SHG signals, specifically, ζ from (s, s) or (p, s), ∂_{15} from (q, s), ∂_{31} from (s, p), and ∂_{33} from (p, p). Thus, the SHG response from the Si(001) surface is fully characterized by this set of measurements.

If there is a dc electric field along the surface normal, SHG has an additional source from the EFISH effect, as shown in Chapter 2. The surface EFISH effect can be effectively combined into the field-independent surface SHG effect by defining a new set of elements, ∂_{31}^d , ∂_{33}^d , and ∂_{15}^d , and then adding them to the original field-independent elements one by one, written as $\partial_{31} + \partial_{31}^d$, $\partial_{33} + \partial_{33}^d$, and $\partial_{15} + \partial_{15}^d$.

Therefore, the surface EFISH effect is isotropic for the (Si(001) surface. The bulk EFISH polarization is treated by introducing additional tensor elements, ζ^d , η^d , and γ^d . SHG from the bulk EFISH effect is still isotropic for the Si(001) surface. However, it is not appropriate to combine it into either bulk or surface field-independent effect, because ζ^d and η^d have no equivalents in field-independent elements. Moreover, the presence of the EFISH effect greatly complicates the separation of different SHG contributions.

5.3 Experimental conditions and sample preparation

The experimental setup is described in Chapter 1. Four samples were prepared from the same undoped silicon wafer ($\rho > 20\Omega \text{ cm}$), $\langle 100 \rangle$ oriented. The natively oxidized Si (NO-Si) and the thermally oxidized Si (TO-Si) samples are the same as in Chapter 3. Two MOS structures were prepared by depositing Cr on oxidized Si substrates to form Cr coated NO-Si (Cr-NO-Si) and Cr coated TO-Si (Cr-TO-Si), with both Cr coatings 1.5 nm thick. The Cr coating was performed in an Edwards Auto 306 vacuum chamber ($\sim 1 \times 10^{-6}$ Torr) using thermal evaporation. The substrate temperature was kept at 20~45 °C during deposition.

5.4 Experimental results

5.4.1 Comparison of RA-SHG from Cr-SiO₂-Si and SiO₂-Si surfaces

At a two-photon energy of 3.40 eV (fundamental wavelength 730 nm), the RA-SHG signals from the Cr-NO-Si and Cr-TO-Si samples are shown in Fig. 5.1, and those from the NO-Si and TO-Si samples are shown in Fig. 5.2, for (p, p) , (s, p) , and

(q , s) polarization configurations. All these patterns show a fourfold symmetry, but the RA-SHG signals from Cr coated and uncoated samples consistently differ in peak locations for all these polarizations. The (p , p) RA-SHG signal shows a valley at $\phi=45^\circ$ for Cr coated samples while a peak for uncoated samples. The SHG signal from the NO-Si is stronger than that from the TO-Si, while this relation reverses after the Cr coating. Clearly, the Cr coating produces a large change in the RA-SHG response compared to that before coating. The question arises here whether the Cr coating process affects the structure at the SiO₂-Si interface. Based on the deposition condition of thermal evaporation at room temperature, such a possibility is not likely. An additional way to check this is to vary the thickness of the SiO₂ layer on Si(001) surfaces and measure the RA-SHG signal from each sample. A series of oxidized Si(001) surfaces with oxide thickness up to 40 nm were prepared and it was found that the peak locations of the (p , p) RA-SHG signals are all consistent with the observed trends, which further demonstrate that the Cr coating does not affect the structure at the SiO₂-Si interface.

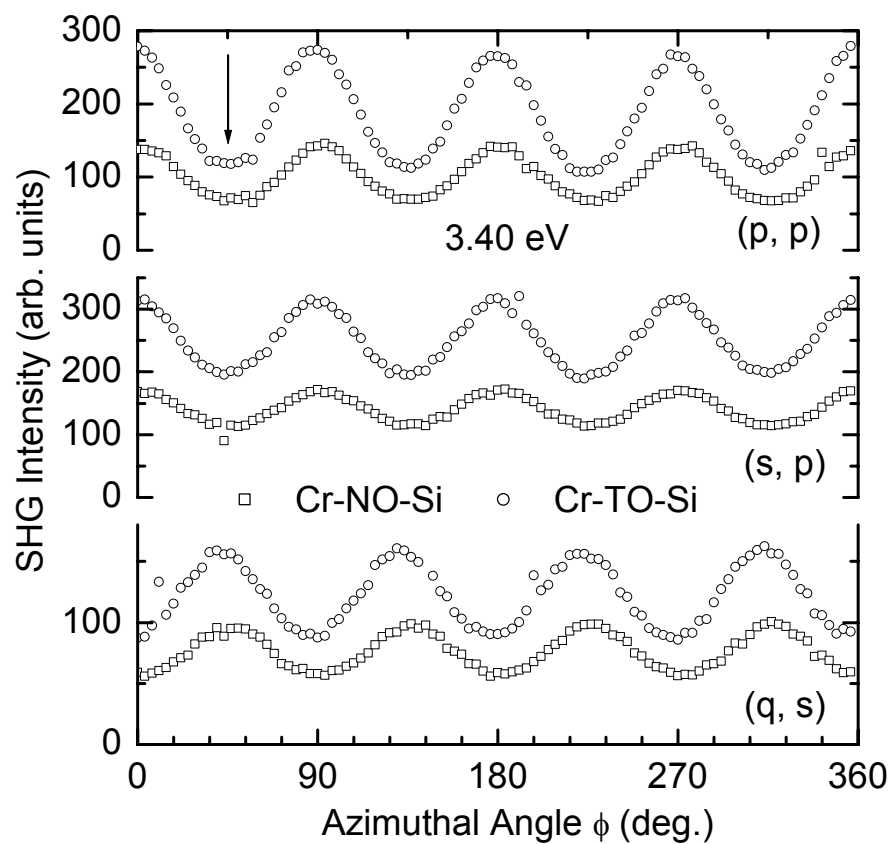


Fig. 5.1. RA-SHG signals from Cr-NO-Si and Cr-TO-Si samples for the (p, p) , (s, p) , and (q, s) polarizations at a two-photon energy of 3.40 eV.

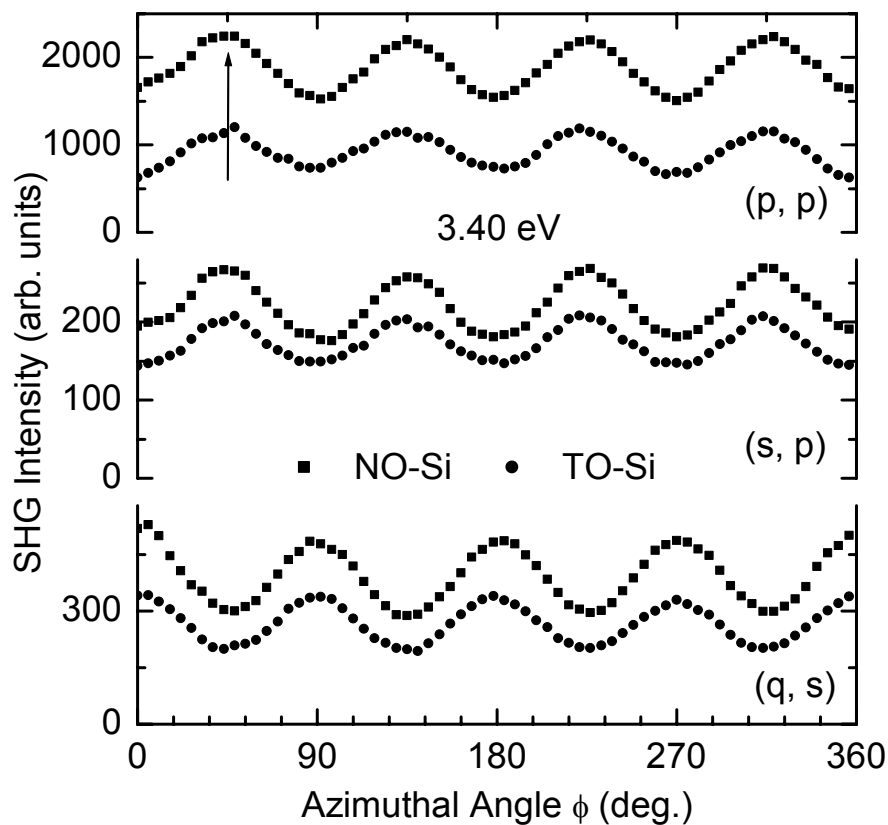


Fig. 5.2. RA-SHG signals from both NO-Si and TO-Si samples for the (p, p) , (s, p) , and (q, s) polarizations at a two-photon energy of 3.40 eV. Note that the peak locations are different from that of Cr coated samples consistently for all these polarizations.

Besides the difference in the peak locations of RA-SHG, the SHG intensities are also very different, especially in the case of (p, p) polarization. However, we should keep in mind that the thin Cr layer changes the linear optical properties at the outside surface of the oxide, which is verified by the comparison of the (p, s) RA-SHG signals from the TO-Si and Cr-TO-Si samples, as shown in Fig. 5.3. The (p, s) RA-SHG signals from the NO-Si is also weaker than that from the Cr-NO-Si (data not shown). Based on the phenomenological theory in Chapter 2, bulk SHG is the only contribution to observed SHG signals. The bulk Si is untouched by surface coating. The weaker SHG signal from Cr coated samples is easily understood to be caused by decreased transmission of both the fundamental and the SHG light through the coating layer, which also suggests that comparison of SHG intensities before and after the Cr coating should take into account of linear optics effects.

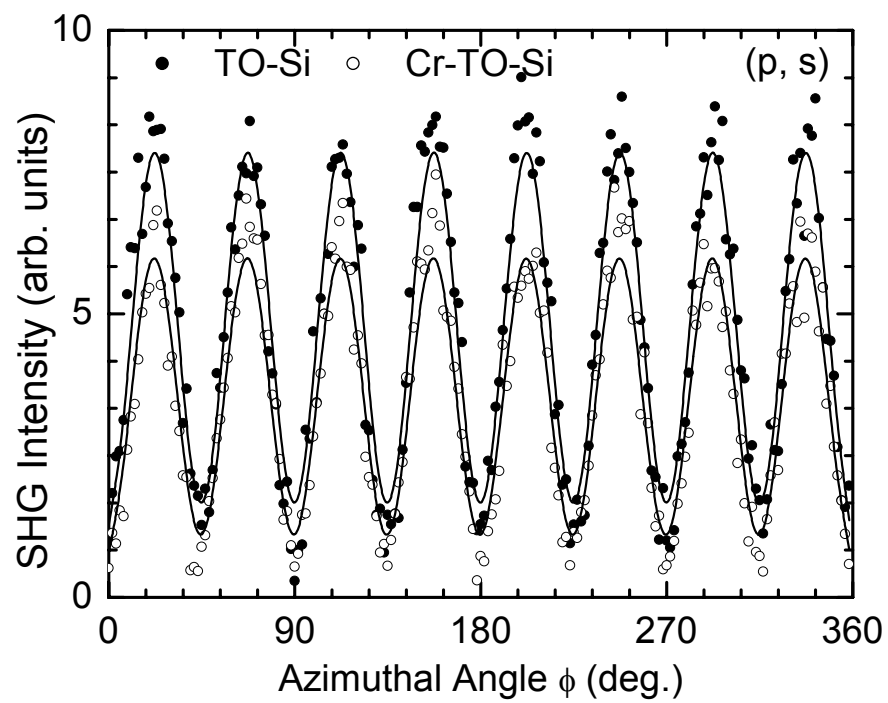


Fig. 5.3. Comparison of the (p, s) polarized RA-SHG signals from TO-Si and Cr-TO-Si samples at a two-photon energy of 3.40 eV. The solid lines show the fits.

5.4.2 Spectroscopic study of RA-SHG from Cr-SiO₂-Si

The relationship of the peak positions in the RA-SHG signals for Cr coated and uncoated samples does not stay the same with variation of the photon energy. The (p, p) RA-SHG signals from the Cr-TO-Si samples at several two-photon energies are shown in Fig. 5.4. At the azimuthal angle $\phi=45^\circ$, RA-SHG signals show a valley at higher photon energies but a peak at lower photon energies. The RA-SHG signal has eightfold symmetry at the two-photon energy 3.28 eV (fundamental wavelength 755 nm), which is significant because absolute SHG intensity is not needed to see the eight peaks. A similar trend is observed for the Cr-NO-Si sample, but the photon energy where the eightfold symmetry appears slightly shifts to blue (data not shown). We showed in Chapter 3 that the peak locations of the (p, p) RA-SHG signals from both the NO-Si and TO-Si samples does not change in the two-photon energy range of 3.06-3.54. This inconsistency in peak locations clearly indicates that the Cr layer affects the spectroscopic behavior of SHG compared to before coating.

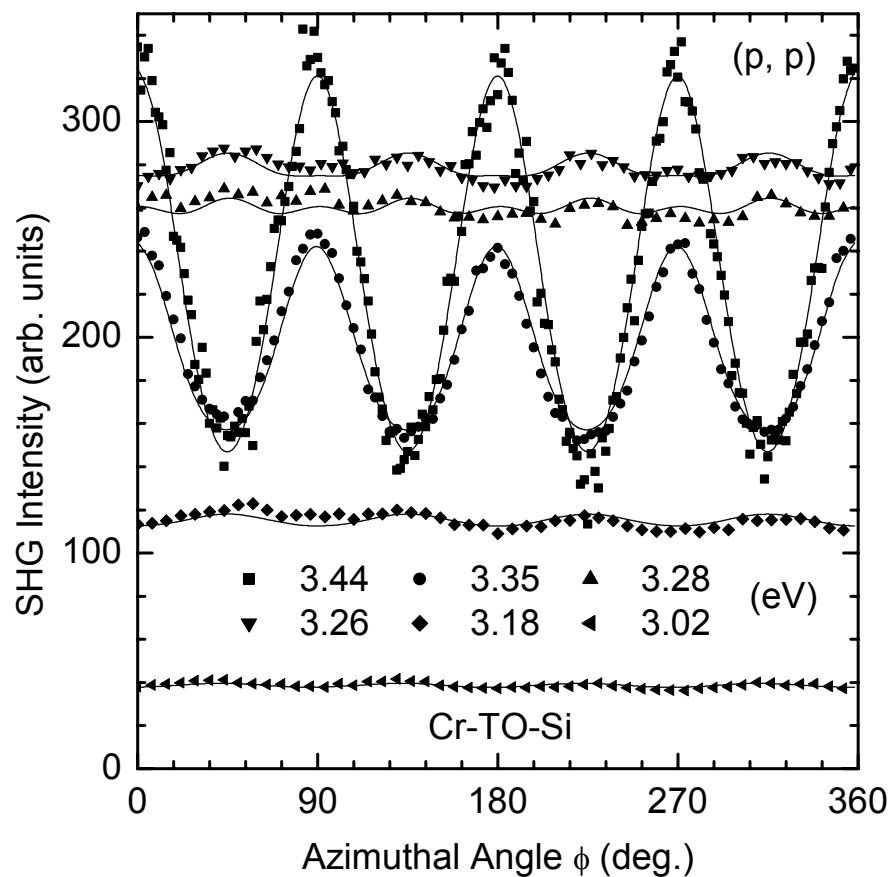


Fig. 5.4. (p, p) polarized RA-SHG intensities from the Cr-TO-Si sample at several two-photon energies. Note that the RA-SHG with eightfold symmetry appears at the two-photon energy of 3.35 eV. Note that these curves are different from the RA-SHG signal from the TO-Si sample for corresponding photon energy.

5.4.3 Comparison of the TD-SHG responses

The Cr coating significantly changes the time-dependent SHG (TD-SHG). Figure 5.5 shows the comparison of the (p, p) TD-SHG signals from all four samples at a two-photon energy of 3.40 eV. To observe the TD-SHG, we moved the sample so that a fresh spot, i.e., one that the laser beam has been kept away for a long period of time, was used for each measurement. Using the shutter, we started to illuminate the sample at time zero and then began recording the signal over a series of 0.5 sec counting intervals. After 80 sec, when the signal was close to its asymptotic value, the shutter was closed. To observe the variation of the SHG signal with time when the laser beam is blocked, we repeated the following procedure. After 30 sec, the shutter was opened for a 0.5 sec gate and the SHG signal was recorded and then shutter was closed again. At the initial charging stage, the TD-SHG signals increase with time for samples without coating while they decrease with time for Cr coated samples. During the measurement, the sample azimuthal angle was fixed at a peak RA-SHG signal for each sample. We note that these trends of increase and decrease in the TD-SHG signals are the same at all other azimuthal angles. The measured time-dependent effect for the (p, s) TD-SHG is negligible for all of the samples.

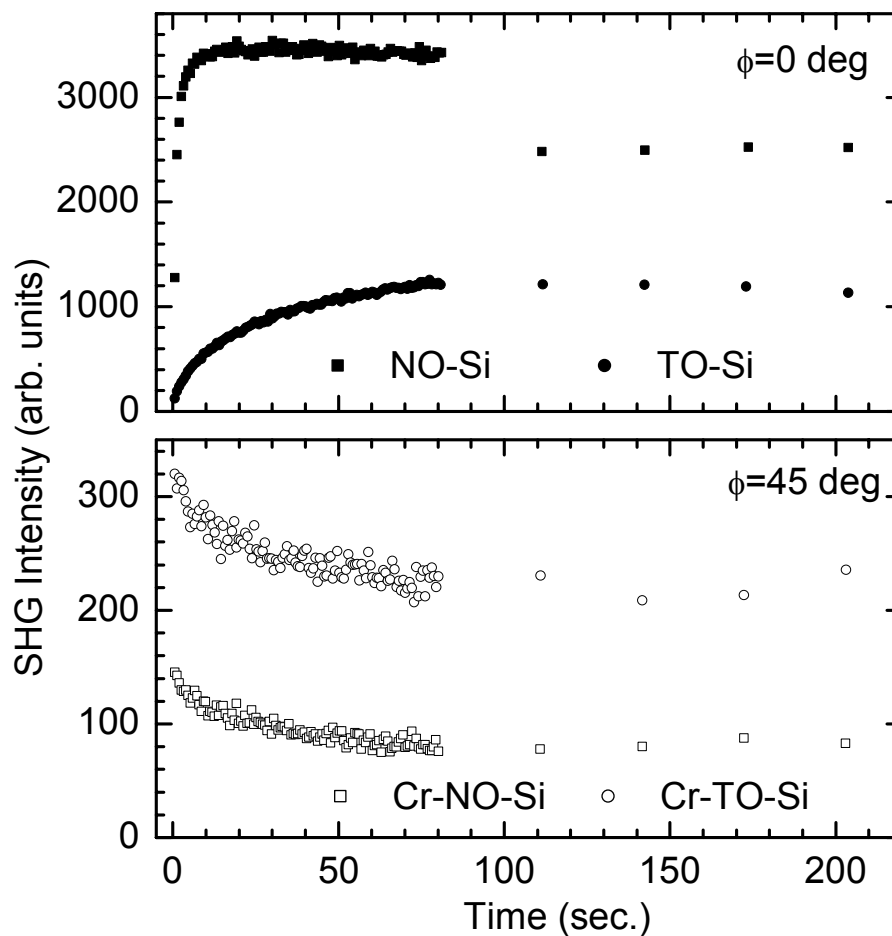


Fig. 5.5. Comparison of the TD-SHG signals for the (p, p) polarization at a two-photon energy of 3.40 eV for different samples: NO-Si and TO-Si (upper panel); Cr-NO-Si and Cr-TO-Si (lower panel). Note that the sample azimuthal angle is chosen to be where the RA-SHG signal shows a peak, i.e., $\phi=0$ deg for uncoated samples and $\phi=45$ deg for Cr coated samples.

5.5 Discussion and further experimental results

5.5.1 Phase inversion due to additional SHG sources

The observed azimuthal dependence of the SHG intensity follows directly from the phenomenological prediction based on symmetry consideration. As shown in Eqs. (5.1), (5.2), and (5.3), the peaks and valleys in the RA-SHG signal comes from interference between isotropic and anisotropic SHG contributions. The latter originates from only the bulk and is independent of surface preparation; therefore, it serves as a reference for both the phase and the amplitude of surface SHG, as we showed in Chapters 3 and 4. We split the isotropic coefficient, a_0 , in Eqs. (5.2) and (5.3) into a real part and an imaginary part, written as $a_0 = a_{0,r} + ia_{0,i}$, and designate them as interfering and non-interfering isotropic SHG contributions, respectively. They are so named because only the real part interferes with the bulk anisotropic SHG contribution, while the imaginary part functions as an azimuthal independent increase in the SHG signal. For the (p, p) polarization, the isotropic SHG is usually much stronger than the anisotropic SHG, thus the RA-SHG scan usually shows fourfold symmetry. If $a_{0,r}$ and a_4 are the same sign, a valley appears at $\phi=45^\circ$ in RA-SHG, and if $a_{0,r}$ and a_4 are opposite in sign, a peak appears at $\phi=45^\circ$. If $a_{0,r}=0$, the RA-SHG is eightfold symmetric, as shown in one the RA-SHG scans in Fig. 5.4. Compared with the eightfold symmetry in the (p, s) RA-SHG, the dc level of the RA-SHG signal on which the modulation rides is much higher for the (p, p) polarization than that for the (p, s) polarization, which is about zero for the latter. It should be

noted that the measured peak locations of the (p, p) RA-SHG signal from Cr coated samples at the two-photon energy 3.40 eV is consistent with previous SHG results on a similar MOS structure at zero dc bias [69] but inconsistent with our results on uncoated samples in Chapter 3.

5.5.2 Further experiments to determine the sources of SHG

In order to investigate the reason for such an apparent difference of the SHG responses from the surfaces of Cr coated and uncoated samples, we prepared a series of new samples to detect possible SHG sources from silica, Cr, and Cr-Silica interfaces. Figure 5.6 shows the results of the SHG signals from different samples at several two photon energies. Based on previous results of SHG on metal surfaces [77, 78], it is reasonable to predict that the Cr layer might introduce an additional SHG contribution. The first sample, designated as Silica, was a 1mm thick fused silica slab without Cr coating. The measured SHG signal in reflection from it is very weak (not shown in Fig. 5.6). The second sample, designated as Cr-Silica, was prepared by coating a 1.5 nm thick Cr film on top of the fused silica sample, using the same coating condition as that for the Cr coated Si samples. The measured SHG signal from the Cr-Silica surface is about two orders of magnitude stronger than that from the Silica surface. This is a clear evidence that the Cr coating has an effect on the total reflected SHG signal; however, we should expect that the additional SHG signal originated from the Cr coating on the Cr-TO-Si is even stronger than the measured SHG signal from the Cr-Silica sample, because Si substrate reflects much more SHG light than silica does, due to different indices of refraction between Si and silica. The third sample, designated as Cr, was prepared by depositing a 125 nm thick Cr film on

a 0.16 mm thick fused silica substrate. The measured SHG signal in reflection from the upper surface of the Cr film is very strong, as shown in Fig. 5.6. Because the thick Cr layer is opaque, light can not penetrate to the Cr-Silica interface, thus no SHG signal is generated from it. This signal is strong, but we should consider that the SHG response from a 1.5 nm thick Cr film is different from that from a very thick Cr film. The trend of increasing SHG signal with increasing coating thickness is expected to be similar to previously measurements on silver films [78]. To study the SHG response from the Cr-Silica interface, we just turned over the Cr sample (125 nm thick Cr coated on a 0.16 mm thick silica substrate) and measured the SHG signal in reflection from the upper surface of silica, which we designate as Silica-Cr. As shown in Fig. 5.6, this signal is about one order of magnitude weaker than that from the Cr sample; however, we expect to see similar SHG signals from Silica-Cr and Cr surfaces. Differences in interfacial morphology and electron mobility between these two interfaces are possibly responsible for the discrepancy. Combining these facts, we conclude that the Cr coating adds an SHG contribution to original SHG from samples without the Cr coating and the outermost surface of Cr film is likely the main source of additional SHG. The change of peak locations in RA-SHG signals at the two-photon energy 3.40 eV is caused by interference effect from additional SHG sources.

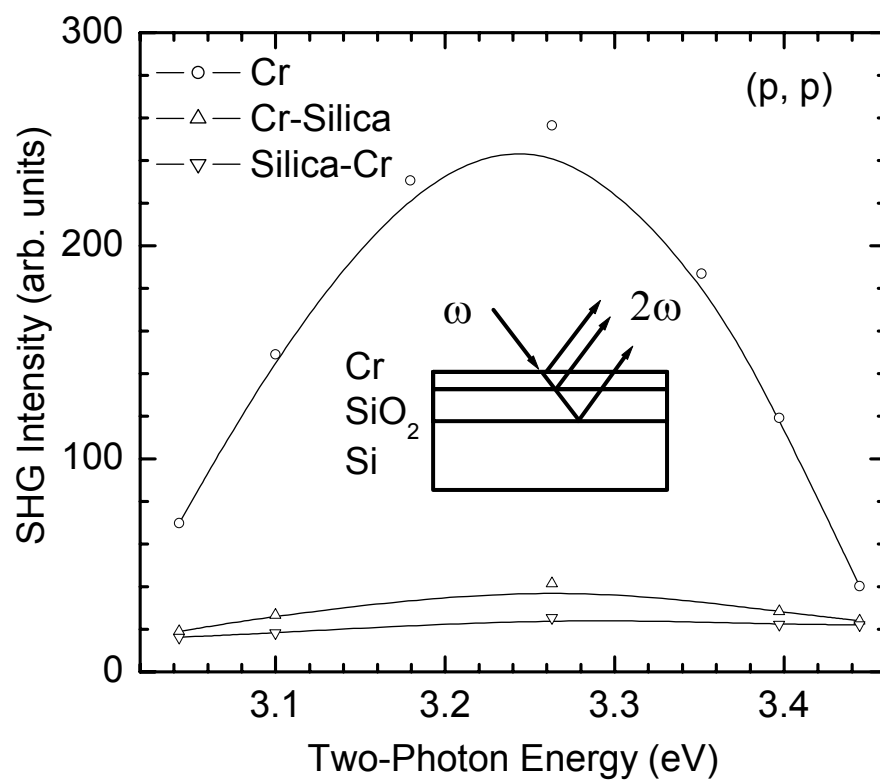


Fig. 5.6. Isotropic SHG signals from the surfaces of a thick Cr film, a thin Cr coated silica sample, and a silica covered Cr sample at different two-photon energies. The inset shows that the measured SHG signal is an interfering combination of different sources.

With the additional sources of SHG from Cr coated samples compared to uncoated samples, an additional concern for the SHG response from MOS structures is whether the bias dependence of SHG originates from the additional SHG sources or original ones. If an external bias voltage is applied between the Cr film and an electrode underneath the Si substrate of the MOS structure, an electric field is applied both across the Cr-SiO₂ interface and the SiO₂-Si interface. To study the bias dependence of the SHG at the Cr-SiO₂ interface, we attached a copper foil on top of a silica slab that has a 125 nm thick Cr film on the backside. A capacitor was formed between the copper foil and the Cr film. A small hole was left in the middle of the copper foil so that both the incident and SHG light were able to travel through it without being affected by the copper foil. The SHG signal was measured in reflection from the silica side through the hole. Up to 40 volts of dc voltage between the Cr film and the copper foil was applied, but a change in the SHG signal with and without the dc bias was not observable, even when the thickness of the SiO₂ was decreased from 1 mm to 0.16 mm. Further experiments is needed to investigate the SHG response under a stronger dc field across the Cr-SiO₂ interface, but the field used here is comparable to previous used values, at which the bias dependence of the SHG signal was observable [71]. Therefore, these previous results [37, 69-71] of SHG on MOS structures characterized the bias dependence of the SHG signal at the SiO₂-Si interface, but SHG signals originated from other unwanted sources were involved in the measured RA-SHG.

By spectroscopic comparison of RA-SHG signals from Cr coated and uncoated samples, we obtain the relative strength of the SHG contribution arising

from the Cr coating. As shown in Fig. 5.4, the SHG signal at $\phi=22.5^\circ$ is only due to the isotropic SHG signal, which peaks at the two-photon energy 3.26 eV nm for the Cr-TO-Si sample. This energy is a significant shift from our earlier result of 3.35 eV for the TO-Si sample in Chapter 3. The SHG signal from the Cr sample also varies with photon energy, as shown in Fig. 5.6. Exact separation of different SHG sources is difficult due to interference among different SHG fields, and the involvement of additional sources of SHG complicates the interpretation of spectroscopic results. At higher photon energy, the effect of the Cr coating on the RA-SHG signal is very strong; while at lower photon energy, it appears to be negligible. Figure 5.4 also shows that the SHG spectrum from Si(001) surfaces strongly depends on the azimuthal angle at which the SHG signal is taken.

5.5.3 Insight into the Charge Trapping Process

The observed trends in the TD-SHG signals can be explained in terms of the self-induced EFISH effect. The dc electric field across the SiO₂-Si interface is not an external field but an effective field, which arises from charge transfer by photon injection and subsequent trapping in the charge traps at the SiO₂-Si interface and inside of the bulk oxide [66, 76]. Comparing the RA-SHG signals in Figs. 5.1 and 5.2, we find that the peak locations for Cr coated samples fall into the valley locations for uncoated samples consistently for all of the (p, p) , (s, p) , and (q, s) polarizations, which suggests that each field-independent element in ∂_{31} , ∂_{33} , and ∂_{15} is roughly out of phase for Cr coated and uncoated samples. We should note that the RA-SHG signals were taken with a counting gate time of 1 sec and after the samples were fully

discharged. The direction of the effective dc field is the same for both the Cr coated and uncoated samples, because electrons transfer out of the Si substrate in one direction. Therefore, the self-induced EFISH effect enhances the TD-SHG signal for uncoated samples while it diminishes the TD-SHG for Cr coated samples. This explains the increasing SHG signals with time from the NO-Si and TO-Si surfaces while decreasing SHG signals from the Cr-NO-Si and Cr-TO-Si surfaces, as shown in Fig. 5.5. The saturated TD-SHG signal is much stronger for NO-Si than for TO-Si, but it is stronger for Cr-TO-Si than for Cr-NO-Si. These results can be understood in terms of the fact that the number of charge traps at the interface between silicon and native oxide is much denser than that after the high temperature thermal oxidation, consistent with other results [79]. The much shorter rise time of the TD-SHG signal for NO-Si compared with TO-Si is due to higher mobility of the hot electrons for NO-Si. No noticeable variation of the (p, s) TD-SHG signal with time indicates that the charge sources come from a very shallow region underneath the interface, compared with the estimated ~ 30 nm escape depth of the SHG light in silicon. In the circumstance of the self-induced EFISH effect, the bulk EFISH source predicted in Chapter 2 is negligible. However, if there is an external dc electric field across a MOS structure, the EFISH effect possibly includes both surface and bulk sources. If the dc field flips its sign, the EFISH field inverts its phase; therefore, peaks of the RA-SHG signal can turn into valleys by applying a dc bias. This explains previous results of bias-dependent RA-SHG signals from Si(001) MOS structures [69, 71].

Comparison of the time-dependent SHG responses between thin and thick oxidized and between Cr coated and uncoated samples allows insight into the carrier

dynamics at interfaces. Previous results suggested that electrons can be injected from the Si substrate to the ambient-SiO₂ interface by a multi-photon process [80-82] and trapping of electrons can be enhanced by using oxygen ambient [66, 83]. An assumption used in these studies is that the electron band structure of the SiO₂ overlayer remains unchanged with decreasing oxide thickness. When the thickness of the SiO₂ insulator is reduced below 3-4 nm, high tunneling currents could be significant in MOS structures. This indicates that using only the band structure of thick SiO₂ to explain the charging dynamics is not applicable to ultrathin SiO₂ films. Another assumption is that the SHG contribution at the ambient-SiO₂ interface is negligible, which is based on the fact that the SHG signal from a thick silica substrate held in air is negligible compared with that from the Si surface, as shown by earlier results [84] and by our results in this chapter. However, if the SiO₂ overlayer is very thin and if there are trapped electrons inside the oxide and at the ambient-SiO₂ interface, considerable SHG signals could be generated from both sources. Previous observed dramatic decrease of the SHG intensity from a metal surface with increasing pressure of ambient oxygen is a clear evidence of ambient influence on SHG [85]. We used N₂ ambient but observed strong TD-SHG signals. This indicates that the charge traps are not likely located at the ambient-SiO₂ interface because N₂ is very inert and its potential for charge trapping is small. If the ambient is changed from N₂ to O₂, we found little change in the TD-SHG signal for the TO-Si but dramatic change for the NO-Si. If electrons can tunnel across the thin SiO₂ overlayer by one photon injection, or if the charge traps are located at the SiO₂-Si interface, then a multiple photon process is not likely to happen. For ultrathin oxide covered Si

samples, further experiments are needed to identify whether the enhancement of the SHG signal by oxygen ambient is caused by more charge traps compared to that of the N₂ ambient or caused by an additional SHG source at the O₂-SiO₂ interface. We also found that the TD-SHG signals from both the Cr-NO-Si and Cr-TO-Si samples show similar noticeable change if the ambient is changed from N₂ to O₂, which can be understood to be due to the same ambient-Cr interface. These results probably suggest that if there are free electrons at the ambient-medium interface, the effect of oxygen ambient on SHG is strong, otherwise it is negligible.

5.6 Summary

The combination of polarization selection and RA-SHG has been applied to study the effect of the ultrathin (1.5 nm) Cr coating film on SHG from Cr-SiO₂-Si(001) structures with either native oxide or thermal oxide gate insulators. By comparing RA-SHG signals from Cr coated and uncoated SiO₂-Si(001) surfaces, we find that the peak locations of the signal as a function of sample azimuthal angle are different at a certain photon energy consistently for several polarizations. This enabled a detailed spectroscopic comparison of the RA-SHG signals from the Cr coated and uncoated samples, which reveals that the peak locations are different for higher photon energies while the same for lower photon energies. In addition, we have shown that the TD-SHG signals decrease for Cr-coated samples and while increase for uncoated samples. These results indicate that the Cr coating has a significant effect on the SHG from Cr-SiO₂-Si(001) structures. Through further investigation, we have identified that the Cr coating introduces additional sources of SHG, of which the most important contribution is from the outermost surface of the

Cr film. The SHG intensity strongly depends on the thickness of the overlayer oxide. For the same thinner overlay oxides, we have observed stronger SHG signal for uncoated samples but weaker SHG signal for Cr coated samples. All these results have been well explained by using a phenomenological theory that takes into account of crystal symmetry and self-induced EFISH effect. In several previous studies [37, 69-71], the Cr-SiO₂-Si(001) MOS structures were used to study the properties of the SiO₂-Si interface and the SHG arising from the Cr coating was neglected. However, we showed here that the Cr coating significantly changes both the spectroscopic and the time-dependent behaviors of SHG by interfering with additional SHG sources introduced by the ultrathin Cr coating.